



Compliance and port air quality features of ship fuel switching regulation: by a field observation SEISO-Bohai

Yanni Zhang^{1,2,*}, Fanyuan Deng^{1,2,*}, Hanyang Man^{1,2,*}, Mingliang Fu^{1,2,3}, Zhaofeng Lv^{1,2}, Qian Xiao^{1,2}, Xinxin Jin^{1,2}, Shuai Liu^{1,2}, Kebin He^{1,2}, Huan Liu^{1,2}

- 5 ¹State Key Joint Laboratory of ESPC, School of Environment, Tsinghua University, Beijing 100084, China
²State Environmental Protection Key Laboratory of Sources and Control of Air Pollution Complex, Beijing, 100084, China
³State Key Laboratory of Environmental Criteria and Risk Assessment (SKLECRA), Chinese Research Academy of Environmental Sciences, Beijing, 100012, China
*These authors contributed equally to this work.
- 10 *Correspondence to:* Huan Liu (liu_env@tsinghua.edu.cn)

Abstract.

Since January 1st, 2017, ships berth at the core ports of three designated Domestic Emission Control Area (DECA) in China should use fuel with sulphur content less than or equal to 0.5 %. In order to evaluate the impacts of switching fuel, a measurement campaign (SEISO-Bohai) was conducted from 28 December 2016 to 15 January 2017 at JingTang Harbor, an area within the 7th busiest port in the world, including meteorological monitoring, pollutants monitoring, aerosol sampling and fuel sampling. During the campaign, 16 ship plumes were captured by the on-shore measurement sites, and 4 plumes indicates the usage of high S_F fuel. The average reduction of average $\Delta\text{NO}_x/\Delta\text{SO}_2$ ratio from high sulphur plumes (3.26) before January 1st to low sulphur plumes (12.97) after January 1st shows a direct SO₂ emission reduction of 75 %, consistent with the sulphur content reduction (79 %). Average concentrations of PM_{2.5}, NO_x, SO₂, O₃ and CO during campaign were 147.85 $\mu\text{g}\cdot\text{m}^{-3}$, 146.93 ppb, 21.91 ppb, 29.68 ppb and 2.21 ppm, respectively, among which NO_x reached a maximum hourly concentration of 692.6 ppb and SO₂ 165.5 ppb. Mean concentrations of carbonaceous and dominant ionic species in particles were 6.52 (EC), 23.10 (OC), 22.04 (SO₄²⁻), 25.95 (NO₃⁻) and 13.55 (NH₄⁺) $\mu\text{g}\cdot\text{m}^{-3}$. Although the carbonaceous species in particles were not significantly affected by fuel switching, the gas and particle pollutants in ambient air exhibited clear and effective improvements from implementation of low sulphur fuel. Comparison with the prevailing atmospheric conditions and wind map of SO₂ variation concluded the prompt SO₂ reduction by 70 % in ambient air after fuel switching. Given the high humidity in site, this SO₂ reduction will abate the amount of secondary aerosols and improve the acidity of particulate matter. Based on enrichment factors of elements in PM_{2.5}, vanadium was identified as marker for residual fuel ship emissions, decreasing significantly by 97.1% from 309.9 $\text{ng}\cdot\text{m}^{-3}$ before fuel switching to 9.1 $\text{ng}\cdot\text{m}^{-3}$ after, which indicated a crucial improvement due to the implementation of low sulphur fuel. Ship emissions were proven to be significantly influential both directly and indirectly on port environment and coastal areas around Bohai Bay, in where the population density reaches 650 per square kilometre. The results from this study provide positive impact on air quality of fuel switching and indication of new method on identification of ship fuel type.



1 Introduction

Maritime transport is a globally important source of pollutants, and thus one of the well-established culprit of adverse effects of ship emissions on air quality (Eyring et al., 2010; Endresen et al., 2003; Eyring et al., 2005; Fridell et al., 2008; Jalkanen et al., 2009; Liu et al., 2016; Viana et al., 2014), climate (Lauer et al., 2007; Tronstad Lund et al., 2012; Liu et al., 2016) and human health (Campling et al., 2013; Corbett et al., 2007; Winebrake et al., 2009). Estimation shows that ships contribute 15 % of global NO_x emissions and 4-9 % SO₂ as well (Eyring et al., 2010). In Europe only, ships in 2005 emitted 2.8 million tons NO_x, 1.7 million tons SO₂ and 0.2 million tons PM_{2.5}, around 20 % of land-based contribution (Campling et al., 2013). According to the United Nations Conference on Trade And Development (UNCTAD, 2018), the volume of world seaborne trade has continually grown by 66 % from 2000 to 2015. As global commerce expands, ocean-going vessels consume more fuels but generally the low-quality residual fuels containing high amount of sulphur and heavy metals (Lack et al., 2011), which differs greatly from inland fuel usage. In China, the average sulphur content of marine fuel (S_F) was 2.43 % (by mass, i.e., 24300 ppm) before regulation (Liu et al., 2016), extremely higher than the sulphur content restriction 10 ppm applied for inland fuel (China National Standard GB 19147-2013 and GB 17930-2013), leaving ships one of the prominent contributor in major port cities (Lai et al., 2013; HKEPD, 2014; Zhao et al., 2013). In eastern China, ship emissions accounted for an annual increase of up to 5.2 μg·m⁻³ PM_{2.5}, which influenced the air quality in not only coastal areas but also the inland areas hundreds of kilometres away from the sea (Lv et al., 2018).

These situations have constantly drawn attention on coastal air pollution and correlative emission control strategy. The International Maritime Organization (IMO), the European Union and the United States have implemented regulations in an effort to reduce ship emissions, among which the Fuel Quality Regulation has proven potent in many countries for addressing the issue of sulphur oxides (SO_x) and particulate matter (PM) emissions. IMO has regulated S_F on a global scale from current 3.5 % to 0.5 % by 2020, and implemented more stringent legislation in designated emission control areas (ECAs), in which considering SO_x emissions include the Baltic Sea, the North Sea, the English Channel, and coastal waters around the Canada, US and the US Caribbean Sea. The allowed S_F in ECAs was 1 % in 2010 and has shrunk into 0.1 % since 1 January 2015 (IMO, 2008). Estimation shows that IMO limitation of 0.1% S_F in ECAs would reduce SO₂ emissions by 82 % by 2020, and further 23,000 tons of SO₂ and 46,000 tons of NO_x totally by 2030 in European seas (Campling et al., 2013). This assumption was supported by other comparable results from sub-region assessment and in site measurements (Matthias et al., 2010; Viana et al., 2015; Zetterdahl et al., 2016). Likewise, EU Directive 2012/33/EU demands that ships at berth in Union ports use fuels with S_F < 0.1 % since December 2012, which brings about 50 % reduction of PM_{2.5} emissions from ships between 2007 and 2012 in Venice, Italy (Contini et al., 2015). Beginning in July 2009, the US state of California introduced legislations limiting vessels operating within 24 nautical miles (44 km) of the California coastline to switch to marine gas oil (MGO) or marine diesel oil (MDO) with a maximum S_F of 1.5 % or 0.5 %, respectively (by January 2012 S_F shall be < 0.1 %) (CARB, 2009). As a result, clear improvement of air quality was observed at the Port of Oakland and in the surrounding San Francisco Bay



area in 2010 (Tao et al., 2013). Also, Lack et al. (2011) reported that fuel quality regulation along with speed restriction in California could generate an 88% reduction in gaseous and particle pollutant concentrations.

Based on widely acclaimed Fuel Quality Regulations above, China promulgated in 2015 the Implementation of the Ship Emission Control Area in Pearl River Delta, the Yangtze River Delta and the Bohai Rim (Beijing-Tianjin-Hebei area) (MOT, 2015), designing three DECAs with phased S_F requirements. Since 1 January 2017, ships berth at the core port of three DECAs should use fuel with S_F less than or equal to 0.5 %. This newly regulation provides an opportunity to measure the influence of limiting S_F on the magnitudes of ship emissions in China. However, comparing to the fuel regulation after years of enforcement and optimization in Canada, Europe and USA, this one in China was incipient in clauses and vague in terms of supervision. The possible effects of ship emission control are compelling indeed, but also difficult to evaluate due to the variability of complicated local emission sources and complexity of fleet management. Up to now, much of the previous research on the subject of ship emission control has been restricted to limited comparisons of emissions, failing to specify the compliance of vessels or a practical method to indicate it.

In order to explore the method to capture fuel-related emission change and the impact on air quality of switching fuel, we selected the Bohai Rim (Beijing-Tianjin-Hebei) as research area and conducted in situ measurement of meteorological conditions and pollutants along with chemical analysis of sampled fuels and aerosols, which is a series of typical method within the field of measuring air quality. The campaign ran from 27 December 2016 to 15 January 2017, covering the primary period of the newly regulation. By comparing ship emissions and air quality before and after switching fuel, this paper will shed light on the potential emission reduction effects of the enforced regulation. Meanwhile, certain features in ship plumes were found related to fuel type, hence providing another angle of supervising ship fuels in practice. This could be helpful in actual implementation and management of the new regulation.

2 Methodology

2.1 Field measurement

2.1.1 Measurement site

The measurement station (39.204576° N, 119.004028° E) for Shipping Emission and Impacts by Switching Oil in Bohai Bay (SEISO-Bohai) campaign is located at the corner of main navigational channel to the third pool in JingTang Harbor (JT for short), on the property and with the support of Hebei Tangshan Harbor Economic Development Zone Office (Fig. 1). Located in Bohai Bay, JT belongs to the Port of Tangshan, one of the core ports in the designated DECAs. China Port Yearbook (2017) reported a total throughput of 520 million tons in the Port of Tangshan, in which JT undertook over 270 million tons. Population density is high around JT and surround Port Economic Development Area, which is over 650 people per square kilometre. Details of JT is described elsewhere (Xiao et al., 2018). The station consists of a measurement container, meteorological observation on roof and aerosol sampling.



2.1.2 Meteorological monitoring

A small meteorological monitoring station was placed on the roof of the container and obtained temperature (°C), relative humidity (%), wind speed ($\text{m}\cdot\text{s}^{-1}$), wind direction and radiation intensity every 1 min, from 28 December 2016 to 15 January 2017. Abrupt high temperature values were subtracted from results because there was obvious mismeasurement when instrument indicated 40°C for ambient temperature in winter.

2.1.3 Particle and gas monitoring

Continuous concentrations of 6 gases (NO, NO₂, NO_x, SO₂, and O₃ in ppb and CO in ppm) were measured every 1 min and PM_{2.5} and PM₁₀ (in $\mu\text{g}\cdot\text{m}^{-3}$) every 1 hour with a Sailhero XHAQMS3000 air quality continuous monitoring system, from 28 December 2016 to 13 January 2017. Monitoring modules consist of NO, NO₂ and NO_x measurement by an analyser, SO₂ detection by UV fluorometric, CO by IR absorption, O₃ by UV spectrophotometry, and particles by β -ray absorption. The instrument had a short, erroneous measurement at the beginning of the campaign, due to maybe unskilled operation, which resulted in some negative values of gas pollutants and over-exaggerating values of SO₂, CO and O₃. We fixed the instrument immediately and to ensure the accuracy of data, those values above were removed. Mismeasurements of O₃ occurred fitfully during the campaign, appearing as a sinusoid fluctuation below 10 ppb, which were subtracted from the results. It should be mentioned that air quality of Xinli Primary School (XL for short, an official air quality monitor site as shown in Fig. 1) as control group was provided by an official air quality monitor (see in <http://www.aqistudy.cn>).

2.1.4 Aerosol sampling

The campaign resulted in the collection of 14 valid samples in which two parallel samples per day were collected before 31 December 2016 and 1 sample per day after that. The aerosol samples were collected for 23 h (normally from 16:30 to 15:30 LST the next day, local standard time, and named after the ending date) on an 80 mm-diameter pre-fired quartz microfiber filters (CHM QF1 grade) by a Laoying Model 2030 TSP sampler. All samples were put in its original polyethylene plastic box immediately, wrapped in two layers of pre-stoved tinfoil, and then reserved in a refrigerator subsequently. In order to avoid any possible contamination of the samples, all the above procedures were strictly quality-controlled.

2.2 Chemical analysis

2.2.1 Carbon analysis

0.55 cm² section of each aerosol sample and blank filters were measured for concentrations of organic carbon (OC) and elemental carbon (EC) by the Thermal Optical Transmission Method in a DRI 2001 organic carbon/elemental carbon (OC/EC) analyser. OC and EC values were determined through Interagency Monitoring of Protected Visual Environments Protocol (referred to as IMPROVEA method). Samples were heated in a completely oxygen-free helium atmosphere, by four increasing temperature steps to remove all OC on the filter, during which part of OC was pyrolyzed. Then the pure helium eluent was



switched into a 10 % oxygen/helium mixture in the oven and stepped into 800°C for EC determination. OC and EC are detected by a flame ionization detector after oxidation to carbon dioxide and then reduced to methane. The detection limit of this analysis is 0.82 $\mu\text{g}\cdot\text{cm}^{-2}$ for OC and 0.2 $\mu\text{g}\cdot\text{cm}^{-2}$ for EC.

2.2.2 Ion analysis

5 50 cm^2 section of each aerosol sample and blank filters were extracted with 10 ml ultra-pure water in an ultrasonic bath at 4 °C for 30 min. Inorganic ions of Na^+ , NH_4^+ , K^+ , Mg^{2+} , Ca^{2+} , Cl^- , NO_3^- , and SO_4^{2-} were analysed using a DIONEX ICS-2100 ion chromatograph. The ion chromatograph system was firstly calibrated by a standard solution before running samples. Data obtained from a sample was compared to that from the known standard, achieving identification and quantification of sample ions. The detection limit was 0.1 $\mu\text{g}\cdot\text{L}^{-1}$.

10 2.2.3 Element analysis

20 cm^2 section of each aerosol sample and blank filters were digested with 25 ml of an 8 %-HCl/ 3 %-HNO₃ solution in an ultrasonic bath at 69 °C for 3 h. The solutions were cooled, vortex mixed, and then placed in a centrifuge at 2800 rpm for 15 min to settle any insoluble particle, of which a 5 ml aliquot is taken for analysis of 30 elements (Be, Na, Mg, Al, K, Ca, Ti, V, Cr, Mn, Fe, Co, Ni, Cu, Zn, As, Se, Sr, Mo, Ag, Sn, Ba, La, Ce, Hg, Tl, Pb, Th and U) by an X Series 2 ICP-MS mass spectrometer. Measured Be concentrations were mostly 0 $\mu\text{g}\cdot\text{m}^{-3}$ during the whole sampling, which was subtracted from results. Cr was also removed since the blank value exceeded most of the sample results. Several concentrations of Cd and Mo were below detection, which was removed as well.

2.3 Ship plume event

Method of identifying *ship plume event* using direct and simultaneous measurements of trace gases with in situ instruments aims at the surveillance of emissions and fuel type on board of passing ships. Since the measurement site is in the vicinity of the channel and the berth, when wind directions are favourable for measurements, ship plumes passing the instrument leave a distinctive change of the measured components against background concentrations, which is defined as the *ship plume event*. Several studies have confirmed that synchronic variation in pollutant concentrations can be used to identify the occurrence of ship plume events in observation near the harbour (Alföldy et al., 2013; Ault et al., 2010; Contini et al., 2015; Gao et al., 2016; Kattner et al., 2015; Lu et al., 2006): SO₂, NO_x, CO₂, BC, PM_{2.5} concentrations and number concentrations of aerosol particle would increase simultaneously at the onset of the ship plume, but O₃ concentration would decrease due to its reduction reaction with NO forming NO₂.

Nitrogen compounds were abundant in JT due to the heavy traffic, while source of large amount of SO₂ emissions was rather simple. Therefore SO₂ peaks, or SO₂ episodes, were used as an indicator for recent anthropogenic emissions. The background SO₂ per day was set as the daily lowest concentration, and any enhancement that was more than 3 ppb was marked as the time stamp of a possible ship emission event. For these time stamps, peaks in NO_x along with simultaneous valleys in O₃ were then



identified in valid data, which resulted in 16 ship plumes. The signals were only affirmed when there were significant peaks and clearly determinable backgrounds. Finally ship plume event were marked if the existence of ships was positive in the upwind direction of those signals. The combination of the trace gas peak time, the wind direction, and the ship traffic information (time of ships leaving and berthing) provided by marine administration in the port will enable the identification of the plume-related ship. For example, a ship plume event was identified in 5 January 2017 from 15:36 to 16:08 (Fig. 2). The timing and conditions associated with each positively identified ship plume event are listed in Table 1.

The ratio of ship-emitted NO_x to SO_2 , i.e., the enhancement of NO_x to SO_2 in observation ($\Delta\text{NO}_x/\Delta\text{SO}_2$), correlates with the fuel type, and rises if ships switch to low sulphur fuel (McLaren et al., 2012; Sinha et al., 2003). In this study, data in ship plume event was averaged every 4 minutes, and the suitable baseline point was set as the background concentration either before or after ship plume event. Then the $\Delta\text{NO}_x/\Delta\text{SO}_2$ ratios were calculated via a two-sided linear least squares regression of NO_2 to SO_2 using all points within each plume event including the baseline point (Fig. 2). This method is similar to that used for determination of emission ratios (McLaren et al., 2012) or emission factors (Williams et al., 2009) in ship plumes.

2.4 Properties of fuel samples

Intermediate fuel oil (IFO), or called heavy fuel oil, is typically used by marine vessels. As being the petroleum product left after distilling all other fractions from crude oil, IFOs have high density, carbon/hydrogen ratio and sulphur content (varying from 2 % to 5 %) compared with gas and oil products used by other means of transportation. In addition, high concentrations of organics, metals and the compounds between are obtained in IFOs from their presence in the original crude oil. IFOs are categorized into IFO380, IFO180 and IFO60 by their maximum viscosity measured at 50 °C, and the fuel quality is relatively better as the viscosity reduces (Table 2). Recent on-board as well as in situ measurements revealed that high S_F fuel generally gives higher sulphur, particle and soot emissions (Celo et al., 2015; Contini et al., 2015; Cooper, 2003; Fridell et al., 2008; Lack et al., 2011; Moldanová et al., 2009; Petzold et al., 2010; Sinha et al., 2003; Winnes and Fridell, 2010; Winnes et al., 2016). Significant metal contribution of residual fuel combustion was also noted (Lake et al., 2004), and the contribution to emission (Kweon et al., 2003; Lack et al., 2011; Lee et al., 1998) and formation (Ault et al., 2010) of particulate organic matter as well.

Research shows ships in SECAs would switch to marine diesel fuel (MDO), a cleaner kind typically used to meet the requirement of many fuel quality regulations and emission limits. Compared to IFOs, MDOs contain lower density, carbon/hydrogen ratio, and content of nitrogen (~10 % of IFOs), sulphur (~30 % of IFOs) and heavy metal (significant reduction) (Table 2). With low S_F , these cleaner fuels prove to be better performance on emissions by promising reduction of emission (Cooper and Gustafsson, 2004) and further reaction of acidification and eutrophication (Bengtsson et al., 2011; Fridell et al., 2008; Sinha et al., 2003). Another record worth mentioning is that hybrid fuels that blend IFO and cleaner fuels to comply with S_F limit are found widely used by ships operating in SECAs (Winnes et al., 2016; Zetterdahl et al., 2016), since the price of distillate fuels is an obstacle for contractors to completely abandon IFOs. As Table 2 shows, content of metals in hybrid fuels are in between that of IFOs and MDOs due to the blending, but density, carbon, hydrogen and nitrogen are



consistent with that of IFOs, indicating a IFO-similar quality which was proven to be less improvement on particle emission and health risk than totally abandoning IFOs (Winnes et al., 2016).

In order to figure out the fuel type ships were to use after implementation in JT, three fuel samples were taken from the three vessels berthed at JT in 14 January 2017, one for each, and sent for analysis of fuel properties and chemical composition according to the petroleum industry standard (SH) and national standard (GB) of China.

2.5 Backward trajectory analysis

Back trajectories were used to identify the origin and potential influences of different source regions on V concentrations during each sampling day. The 24 h back trajectories of the air mass during each sampling day were computed at 500 m a.g.l (above ground level) using the HYSPLIT 4 model (NOAA, 2013). The GDAS meteorological data was used as input.

10 Trajectories began at 08:00 UTC (16:00 LST, consistent with sampling period) and were calculated every 6 h.

2.6 Other parameters

Enrichment factor (EF) was used for general evaluation of influences of anthropogenic sources on elements contents of particles (Zhao et al., 2013). EF is calculated following Eq. (1):

$$EF = \frac{\left(\frac{X}{R}\right)_{\text{aerosol}}}{\left(\frac{X}{R}\right)_{\text{crust}}} \quad (1)$$

15 where $(X/R)_{\text{aerosol}}$ is the concentration ratio of the interest element X to the reference element R in aerosol, and $(X/R)_{\text{crust}}$ is the concentration ratio of X to R in crust. We used the composition of the continental crust from study of Wedepohl (1995) and used Al as the reference element R. Species with EFs less than 10 usually indicate a major crustal source, while species with high EFs probably indicate a significant anthropogenic source.

20 Sulfur oxidation ratio (SOR) and nitrogen oxidation ratio (NOR) are used to elucidate the SO_4^{2-} and NO_3^- contribution (Ohta and Okita, 1990; Ostro, 1995; Wang et al., 2005) according to:

$$\text{SOR} = \frac{[\text{SO}_4^{2-}]}{[\text{SO}_4^{2-}] + [\text{SO}_2]} \quad (2)$$

$$\text{NOR} = \frac{[\text{NO}_3^-]}{[\text{NO}_3^-] + [\text{NO}_2]} \quad (3)$$

25 where square brackets are molar concentrations in units of $\text{mol}\cdot\text{m}^{-3}$. SOR/NOR above 0.1 indicates photochemical redox reaction of SO_2 or NO_x in ambient air. Higher SOR and NOR values indicate larger amounts of secondary sulfates and nitrates formation (Khoder, 2002).



3 Results

3.1 Impacts on port air quality with switching fuel

3.1.1 SO₂ reduction in the polluted port area

The climate of JT is strongly influenced by the sea breeze. Mean value of relative humidity during campaign was 69.4 % (ranging from 21.8 % to 99.9 %), while that of temperature was -0.6 °C. Temperature exhibited a clear diurnal cycle: went lowest before dawn (-2.3 °C), then rose after sunrise (7:00 LST) and reached the highest (14 °C) at 14:00 LST (Fig. 1). Prevailing wind direction was W (23.4 %) and NNW (13.0 %). Wind speed mainly ranged between 1 and 4 m·s⁻¹ (2.7 m·s⁻¹ as average). Coastal meteorological patterns like above play an important role in the dispersion, transformation, accumulation or removal of air pollutants (Gariazzo et al., 2007).

During campaign, the day-to day variation was large due to variation in both complicated sources and removal in JT, but overall data exhibited a heavy polluted environment in JT. As the primary pollutant at site, PM_{2.5} concentrations were used to classify local pollution level. In over 50 % of days, PM_{2.5} concentration was above 115 µg·m⁻³, which is the Grade IV criterion of China's daily Air Quality Standard (HJ 633-2012) (Fig. 3), and the mean concentration during campaign (147.85 µg·m⁻³) was much higher than that of city area in Tangshan (117.9 µg·m⁻³) in the same season (Zhang et al., 2017). The PM_{2.5} concentration was even 3 times the wintertime PM_{2.5} in Hong Kong (Gao et al., 2016), and twice the Yangshan Port, Shanghai (Zhao et al., 2013). This suggests severe air pollution in JT, which is understandable since winter (Dec-Feb) is the most polluted time in Tangshan due to higher emission and unfavourable atmospheric conditions (e.g. lower mixing heights and more frequent temperature inversions). Until the campaign, the PM_{2.5} concentration in the cold season always exceeds 100 µg·m⁻³ since December 2013, when an official air quality monitor station started to operate (<http://www.aqistudy.cn>). The situation indicates the necessity for implementing appropriate measures for particle emission reduction. Gas pollutants were abundant as well in JT due to the heavy traffic. Average concentrations of NO_x, SO₂, O₃ and CO were 146.93 ppb, 21.91 ppb, 29.68 ppb and 2.21 ppm, respectively. NO_x seemed more polluted in the port having a higher maximum hourly concentration of 692.6 ppb during the campaign, while SO₂ reached the maximum of 165.5 ppb. Peak levels of NO_x and SO₂ were mainly linked with ship activities since measurement site was very close to channel and berth. A lower level of O₃ was observed in JT compared to Yangshan Port in Shanghai (Zhao et al., 2013) and a clear diurnal cycle of O₃ was spotted that the concentration rises in daytime (29.18 ppb) and goes downward at night (16.38 ppb). The combined influence of coastal meteorology was responsible in some degree. During daytime, photochemical reactions and transportation from ozone-rich air increase O₃, while reaction with NO and dry deposition at night destroy O₃. Cases show that O₃ can be totally destroyed if NO source is large (Finlayson-Pitts and Pitts, 2000), and as being in a busy port, our data verifies that (e.g. O₃ approximated to 0 ppb at 21:00 LST on 4 January 2017). Peaks of CO and NO_x coexisted in some degree, but overall there was no evident pattern for CO due to much more complex local combustion emissions.

SO₂ level reduced apparently by maximum hourly concentration dropping from 165.5 ppb before 1 January 2017 to 67.4 ppb after with similar vessel activity. Variation in Fig. 4 confirms this distinct reduction in JT. SO₂ exhibited a prompt drop from



77 ppb to 20 ppb on 30 December 2016 compared to the high and steady concentration in XL, the control group from upwind of JT. This SO₂ reduction was mainly attributed to local sources, since JT was under influence of prevailing atmospheric conditions in XL through diffusion and transmission (NO_x and PM_{2.5} covaried in both sites) where SO₂ did little change. More precisely, the reduction was most likely a direct response to the action of switching fuel, compared with all other variables at port. Wind map shows that the reduction of SO₂ was even more comprehensive in almost every wind direction that blew from the navigational channel of JT to our observational site (Fig. 5). As shown in Fig. 1(c), westerly wind blew through the 3rd pool, and the northeasterly wind through the 2nd pool, in both which direction the SO₂ dropped significantly, while on the contrary, in the southwest direction where wind blew from city and road, SO₂ barely changed, indicating steady non-marine anthropogenic emissions. From this perspective, switching fuel in JT indeed resulted in a reduction of around 70 % on ambient SO₂ concentration.

3.1.2 Carbonaceous and ion species affected by marine vessels

Variation of carbonaceous and ion species was depicted in Fig. 6. Mean (range) concentrations of carbonaceous species determined in PM_{2.5} were 6.52 (5.46-7.69) µg·m⁻³ for EC, and 23.10 (9.88-41.60) µg·m⁻³ for OC (OC levels are uncorrected for artifacts from absorption/volatilization of gaseous organic species). Levels of EC and OC were fairly consistent with that of PM_{2.5} collected in the same period in Beijing (Li et al., 2018b). EC is considered as tracer for primary emissions (incomplete combustion), from sources such as ship, vehicle and power plant in our study, which is affected by fuel quality and combustion. However, little variation after fuel switching was observed here due to the complicated contributors in JT. On the contrary, OC concentrations were much higher with large variation, showing a clear prevalence of organic carbonaceous species over EC. Still, no discernible effects of switching fuel was found on OC concentrations.

Being the major long-range transported aerosol components, SO₄²⁻, NO₃⁻ and NH₄⁺ dominated the ionic species, with strong correlations between each other and an average concentration of 22.04, 25.95 and 13.55 µg·m⁻³, respectively. Ca²⁺, Mg²⁺, Na⁺, K⁺ and Cl⁻ are major constituents of sea salt and mineral dust, with an average concentration of 1.10, 0.21, 0.84, 2.10 and 3.90 µg·m⁻³, respectively (Fig. 6). Port-related emissions were proven to be one of the major sources of local emission in JT. Cl⁻ was relative abundant since the Cl⁻/Na⁺ ratio in the aerosol was 4.79, much larger than in the sea salt (1.8), indicating other strong anthropogenic sources like coal combustion (Yao et al., 2002) and biomass burning (Li et al., 2007; Li et al., 2009). Ca²⁺, as an indicator of mineral dust, was higher than that in city area of Tangshan (0.7 µg·m⁻³), which was considered correlative of port activities (load and unload bulk materials). Moreover, the mass ratio of Mg²⁺/Na⁺ (0.27) were higher than the value of 0.12 reported for sea water, suggesting additional magnesium sources such as dolomite containing soil dust, which may be relative to port activities as well. To evaluate the contribution of stationary emissions and mobile emissions towards air pollution (Gao et al., 2011), mean mass ratio of NO₃⁻/SO₄²⁻ in JT was calculated, and the result (1.19) was higher than that of that in city area of Tangshan (0.7), indicating that JT was more affected by mobile sources than city area.

High humidity in JT will promote secondary aerosol formation of local emissions (Yu et al., 2018). Samples were categorized into *polluted day* and *clean day* based on corresponding PM_{2.5} mass concentration for comparison, since the chemical



composition of atmospheric particulate matter are largely affected by prevailing weather conditions (Röösli et al., 2001). The proportion of sulfates and nitrates in polluted days rose from 55 % of clean days to 70 %, showing a large amount of secondary aerosols either by transportation or by formation. Generally, SOR and NOR in JT were higher than that of city area in Tangshan and Beijing (Fig. 7), and increased significantly from *clean day* (0.14 and 0.10 respectively) to *polluted day* (0.48 and 0.37 respectively), suggesting a strong localized photochemical redox reaction. The OC/EC ratio could be used as an indicator for the extent to formation of secondary organic aerosols (Cabada et al., 2004). In this study, the mean OC/EC ratio was 3.58, much higher than that of Thessaloniki port in Greece (Tolis et al., 2015) and Hong Kong (Gao et al., 2016). Ships were likely responsible for this situation since their OC/EC emission ratio (typically over 10) (Celo et al., 2015; Moldanová et al., 2009; Sippula et al., 2014) was much higher than that of on-road diesel engine (typically ranging from 0.25 to 1) (Oanh et al., 2010). Therefore, the localized photochemical reaction and aerosol formation driven by ship emissions were contributing remarkably to air pollution in JT. This shed light in the pollution control of this Harbor that the secondary pollution should be treated by reduction of local SO₂ emission, which can be achieved by reducing ship emission from switching fuel.

3.1.3 Elemental enrichment factors and marker for ship emissions

The ranges and mean concentrations of all measured elements are shown in Fig. 8. Overall, the mass concentrations of Al, Ti, Mg, Fe, Na, K, Mn, V, Ni, Zn and Pb were abundant and they varied largely with sampling time. Samples were categorized into three batches based on the PM_{2.5} limit of AQI level (HJ 633-2012) during sampling, considering the influences of ambient pollution on particulate chemical composition, while one specific sample 2017/01/04 was set as a background/control group due to none ship activity during its sampling time according to provided ship traffic information. Intra-batch comparison was then performed to estimate variation of elements after fuel switching.

Enrichment factor (EF) was used to normalize the observed concentrations of elements and to evaluate influences of crustal and anthropogenic sources. Generally, elements from Ca to K in Fig. 8 mainly come from geological source, thus classified as *crustal elements*. Ca mostly came from stable crustal sources having the lowest EF values. With EF values around 10 without evident temporal variation, elements from Ti to U could have a major local crustal origin such as dust. Regression analysis comparing EF-Na and EF-K revealed a strong correlation with coefficients (R^2) of 0.994, implying a main contribution of marine source. On the other hand, elements Co, Mn and V were moderately (EF<100) and elements from Ni to Se were highly (EF>100) enriched due to the contribution of anthropogenic sources, which all were classified as *pollution elements*. Co could come from various bulk materials carried with harbour areas, as well as Mn, Cu and Zn (Almeida et al., 2012; Moreno et al., 2007). With EF values strongly correlated with each other, Mn, Ti, Cu, As, Sn, Zn, Pb, Hg and Ag would have a same major anthropogenic source, which is likely the traffic pollution. According to tunnel studies (Lawrence et al., 2013; Li et al., 2018a) and in situ measurements (Terzi et al., 2010; Thorpe and Harrison, 2008), Mn, Cu, Sn, Zn and Pb in PM_{2.5} are related to vehicle emissions as well as tire and brake wear. Weckwerth (2001) reported As-enrichment in PM_{2.5} from shaking rusting rails due to passing trains, explaining our observation since our measurement site was in the vicinity of the train rails around the 1st pool. There were not enough values for Mo and Cd to present patterns, however, literature shows that Mo could be a contribution



of diesel exhaust and brake wear (Weckwerth, 2001), and Cd the motor vehicle emissions (Li et al., 2018a). Again, it was proved that JT was more affected by mobile sources, which heavy metals came mainly from.

Marker for ship emissions was crucial, once confirmed, to deduce the variation of ship emissions. There has been a particular focus on Ni and V in PM_{2.5}, since several recent studies have clearly revealed that V and Ni are representative for ship exhaust particles using Aerosol Time-of-Flight Mass Spectrometer (Ault et al., 2010; Healy et al., 2009) and furthermore, higher V levels in ship emissions were found to be associated with the residual fuel combustion instead of the distillate fuel (Agrawal et al., 2008; Celo et al., 2015). In JT, V and Ni were considered mainly from anthropogenic sources, while they were considered crustal elements in city area of Tangshan. This indicated a unique contributor in JT, which is clearly the ships consuming residual fuel. However in this study, Ni was proven less credible for being a residual fuel marker, since the concentration of Ni was even inconsistent between parallel samples collected in the same day. On the contrary, concentration of V, with significant intra-batch decreases in all three pollution level, proved to be highly related to fuel switching, and whereby V was identified as the perfect marker for residual fuel emission in JT.

Chemical composition of MDO/MGOs indicates that V is below detection limit, but PM_{2.5} samples presented existence of V after switching fuel. It suggests that regional transmitted V should not be overlooked. According to back trajectories, during sampling 2017/01/04 when no ship activity existed, air mass in control group went into the Bohai Bay, and then turned back to JT. This air mass was able to bring in particles with a large amount of V from ships cruising in the sea that still used IFO legally, verifying the influence of air transportation on particle content (Fig. 9). Since the pathway would effectively influence the content of air mass, other trajectories were clustered into three typical types based on transport pathways of air masses, each representing continental dominant, marine dominant and mixing airflows, plotted in Fig. 9. V concentration after fuel switching, was 17.4 ng·m⁻³ under coastal airflows (marine and mixing airflow together), much higher than 9.0 ng·m⁻³ under continental airflows, indicating the significant effect of ship emission on coastal areas. As shown in Fig. 9, samples that shared similar transport patterns from Mongolia-Inner Mongolia region were compared to rule out the portion of transmitted V. Results showed ships have switched fuel in advance and most importantly, the implementation of low S_F fuel reduced ship-source V by 97.1% from 309.9 ng·m⁻³ before fuel switching to 9.1 ng·m⁻³ after.

25 3.2 $\Delta\text{NO}_x/\Delta\text{SO}_2$ ratios and indicated fuel type in ship plumes

In this study, ship plume event was used for the surveillance of emissions and fuel type on board of passing ships (see Sect. 2.3). Altogether 16 ship plume events were measured during the campaign, for which the molar $\Delta\text{NO}_x/\Delta\text{SO}_2$ ratios fell in the range of 0.92-17.89 (Table 1). The accuracy of the molar ratios were justified by proving that losses of NO_x and SO₂ in the plumes during the transit time to the instrument was small. Potential losses of NO_x include photolysis at daytime (Makkonen et al., 2012), conversion to NO₃, N₂O₅ and subsequently HNO₃ at night (McLaren et al., 2010), and heterogeneous conversion of NO₂ to HONO on the aqueous surface of the ocean (Wojtal et al., 2011). The furthest berth in the prevailing direction was 1.5 km away from the site indicating a maximum plume transport time of 9 min at the wind speed of 2.7 m·s⁻¹. Using the transport time and a NO_x lifetime of 3.7 h measured in ship plumes (Beirle et al., 2004), we concluded a maximum potential



loss of 4 % NO_x . Also, loss of SO_2 was attributed to heterogeneous reaction to form particle sulfate with equivalent lifetimes, which counteracts the potential for NO_x reactions to bias the $\Delta\text{NO}_x/\Delta\text{SO}_2$ ratios. Therefore, the maximum error in our measured $\Delta\text{NO}_x/\Delta\text{SO}_2$ ratios due to such loss processes is estimated as < 4 %.

Previous inventories, measurements and ship plume studies have proved a direct correlation between S_F and NO_x/SO_2 molar emission ratio, which also help on the determination of critical point in this work. For high S_F fuels (2.43 %), several emission inventories for Bohai Bay indicated that the NO_x/SO_2 emission ratio was between 1.8 and 2.0 (Liu et al., 2016; Song, 2015; Xing et al., 2016), comparable with the ratio of 2.6 observed from residual fuel plumes (Ault et al., 2010). And for 0.5 % S_F fuels, the inventory indicated 10.51 (Liu et al., 2016), which is also comparable with the ratio of 11.6 observed from distillate fuel plumes (Ault et al., 2010). The NO_x/SO_2 emission ratio rises correspondingly with the drop of S_F , but also is affected by ship engine model, load, operation conditions and combustion conditions in practical conditions (McLaren et al., 2012). Thus the variability in the observed $\Delta\text{NO}_x/\Delta\text{SO}_2$ ratios were expected even when ships consumed the same type of fuel.

Considering all the aspects above, we concluded a ratio over 7.5 as a suggestion of fuel with S_F below 0.5 %, otherwise as a suggestion of high and non-compliant S_F , each shown as areas divided by the x-axis in Fig. 10. The y-axis in Fig. 10 stands for the starting of ship fuel regulation within three DECA in the Implementation Plan. The axes make up four quadrants, each representing different scenarios. The ratios in 1st quadrant indicate compliance of ship towards the regulation, and most of them were higher than 10.51, implying the S_F much lower than 0.5 %. Being above the x-axis as well, ratios in the 2nd quadrant also indicate compliance and the action of advance fuel switching before due. Ratios in the 3rd quadrant (plume #1-5) had an average $\Delta\text{NO}_x/\Delta\text{SO}_2$ ratio of 1.92, conform to the emission ratio in inventory (1.82 and 2.0) before the DECA implementation. Ratios in the 4th quadrant indicate usage of high S_F fuel. As shown in Fig. 10, most of plumes indicate compliance with the 0.5 % S_F limit, while there were still some high sulphur plumes occurred. In this case, precise identification of high sulphur plume contributor and reinforcement of supervision are indeed necessary. Generally, SO_2 reduction of average $\Delta\text{NO}_x/\Delta\text{SO}_2$ ratio was 75 % from high sulphur plumes (3.26) to low sulphur plumes (12.97), consistent with the S_F reduction (79 %) and also the reduction of gas SO_2 in ambient air (70 %, in Sect. 3.1.1), which proves the practicability of this method. One uncertain factor for this method is the difficulty on identifying hybrid fuels whose S_F is around 0.5 %. For S_F around 0.5 %, the NO_x/SO_2 emission ratio was observed either way below or consistent with inventory estimate (around 6 in Winnes et al., 2016; around 11 in Zetterdahl et al., 2016), which may be attributed to the diversity of blending IFOs and MDOs. In this way, ships using hybrid fuels were unable to identify and some could be mistaken as non-compliance. Further research is required in this subject.

3.3 Compliance based on the plumes

Test showed that three ships we sampled from in 14 Jan 2017 burned MDOs (Table 2), which was in conformity with the implementation of fuel regulation in JT. There would be obvious benefits such as significant improvements of emissions and air quality once all vessels complied and switched to MDOs or other alternative distillate fuels. Nevertheless, in this act, it is crucial to ensure the compliance of ships, which requires a more convenient and timely method to indicate fuel quality instead of analysing fuel samples.



After identifying low S_F (compliant) and high S_F (potential non-compliant) ship plumes, we matched each plume with certain vessels by the ship traffic information which contains a series of arrival and departure logs to help estimate the time when different ships passed the sampling site. Using the plume conditions, wind direction and ship traffic information to trace the specific source of measured plumes, we noted that most plumes were likely linked to several ships because the wind often
5 blew through the busy pools and navigational channel where many ships were manoeuvring and at berth. For high S_F plume #9, five ships were in berth in the upwind direction and two ships were passing by during the plume time, indicating a mixture of different individual plumes. Similar situation was found for other high S_F plumes, that five at berth and two passing by were matched with plume #10, five at berth and five passing by with plume #12, and four at berth and four passing by with plume #14. In this case, to achieve a comprehensive and accurate surveillance of compliance of individual vessel, a more detailed
10 and precise database of vessel activity such as AIS data is in need.

4 Conclusions and discussion

Field measurement was conducted at the measurement station in JingTang Harbor, including continue monitoring of meteorological conditions and gas and particle concentrations, from 28 December 2016 to 15 January 2017. Samples of $PM_{2.5}$ were collected every day from 28 December 2016 to 11 January 2017. Moreover, three fuel samples were taken from three
15 vessels berthed at JingTang Harbor in 14 January 2017. Profiles of meteorological conditions and pollutants were obtained, and the chemical characterisation of aerosol and fuel samples as well.

Profiles of pollutants exhibited a heavy polluted environment in wintertime of JT. In over 50 % of days, $PM_{2.5}$ concentration was above Chinese national ambient air quality standard class IV limit value ($115 \mu\text{g}\cdot\text{m}^{-3}$, GB 3095-2012). Average concentrations of NO_x , SO_2 , O_3 and CO were 146.93 ppb, 21.91 ppb, 29.68 ppb and 2.21 ppm, respectively, among which NO_x
20 reached a maximum hourly concentration of 692.6 ppb and SO_2 165.5 ppb. Peak levels of NO_x and SO_2 were mainly linked with ship activities since measurement site was very close to channel and berth, and a clear diurnal cycle of O_3 was spotted due to changes of photochemical reactions and transportation. Mean (range) concentrations of carbonaceous species in $PM_{2.5}$ were $6.52 (5.46-7.69) \mu\text{g}\cdot\text{m}^{-3}$ for EC, and $23.10 (9.88-41.60) \mu\text{g}\cdot\text{m}^{-3}$ for OC. SO_4^{2-} , NO_3^- and NH_4^+ dominated the ionic species, with an average concentration of 22.04, 25.95 and $13.55 \mu\text{g}\cdot\text{m}^{-3}$, respectively. Ca^{2+} , Mg^{2+} , Na^+ , K^+ and Cl^- are major
25 constituents of sea salt and mineral dust, with an average concentration of 1.10, 0.21, 0.84, 2.10 and $3.90 \mu\text{g}\cdot\text{m}^{-3}$, respectively. Enrichment factors of elements in $PM_{2.5}$ were used for determination of marker for residual fuel emissions, which was V in this study. Analysis of carbonaceous and ion species revealed that local port-related emissions were one of the major sources of pollution in JT, especially the mobile sources. High humidity in port just added another straw on the polluted air by promoting localized photochemical reaction and secondary aerosol formation of ship emissions. Moreover, the effect of ship
30 emissions were proven wide because the concentration of V, the identified marker for residual fuel emissions, was much higher in coastal areas than continental areas.



After the due in the implementation of low sulphur fuel, three vessels' fuel samples were collected and they were all compliant to the request of switching fuel. Based on previous studies and background in measuring site, ship plume events were identified for convenient surveillance of fuel quality. The $\Delta\text{NO}_x/\Delta\text{SO}_2$ ratios of all 16 ship plumes fell in the range of 0.92-17.89, during which a ratio over 7.5 was identified as a suggestion of fuel with S_F below 0.5 %, otherwise a fuel with high and non-compliant S_F . After due, four plumes indicates usage of high S_F fuel. However, the compliance was difficult to conclude and detailed and precise database of ship location was required. Generally, the reduction of average $\Delta\text{NO}_x/\Delta\text{SO}_2$ ratio from high sulphur plumes (3.26) to low sulphur plumes (12.97) shows a direct SO_2 emission reduction of 75 %, consistent with the S_F reduction (79 %).

Despite the carbonaceous species in particles were not significantly influenced by fuel switching, the gas and particle pollutants in ambient air exhibited clear and effective improvements from the implementation of low sulphur fuel. Comparison with the prevailing atmospheric conditions suggest a prompt SO_2 reduction by 70 % in ambient air after 30 December 2016, which further analysis concluded as a result from reduction of local marine vessel source. Given the high humidity in site, this SO_2 reduction due to switching fuel will abate the amount of secondary aerosols and improve the acidity of particulate matter. As a marker for ship emission, V concentration dropped by 97.1% from $309.9 \text{ ng}\cdot\text{m}^{-3}$ before fuel switching to $9.1 \text{ ng}\cdot\text{m}^{-3}$ after, indicating a significant reduction due to the implementation of low sulphur fuel.

Data availability. Data are available upon request.

Author contribution. YZ mainly participated in chemical analysis and wrote the article, and FD and HM mainly participated in the design and conduct of field measurements, which was considered as equal contribution to this work. MF participated in designing experiments and was responsible for pilot preparations. ZL and QX helped conduct field measurements. XJ and SL contributed to setting instruments. KH provided constructive comments on this research. HL conceived this study and provided guidance on the whole research process as well as manuscript revision.

Competing interests. The authors declare that they have no conflict of interest.

Special issue statement. This article is part of the special issue “Shipping and the Environment – From Regional to Global Perspectives (ACP/OS inter-journal SI)”. It is a result of the Shipping and the Environment – From Regional to Global Perspectives, Gothenburg, Sweden, 23–24 October 2017.

Acknowledgements. This work was supported by the National Science Fund for Excellent Young Scholars (No. 41822505), the National Natural Science Found of China (91544110 and 41571447), Beijing Nova Program (Z181100006218077),



National Key R&D Program (2016YFC0201504), Special Fund of State Key Joint Laboratory of Environment Simulation and Pollution Control (16Y02ESPCT), and National Program on Key Basic Research Project (2014CB441301). We appreciate it that Hebei Sailhero Environmental Protection High-tech Co.,Ltd and Guangzhou Hexin Instrument Co.,Ltd provided the instruments for our observation. We are also grateful for all the help from Sino-Japan Friendship Centre for Environmental
5 Protection and Sinopec Research Institute of Petroleum Processing.

References

- Agrawal, H., Welch, W. A., Miller, J. W., and Cocker, D. R.: Emission measurements from a crude oil tanker at sea, *Environmental Science & Technology*, 42, 7098-7103, 10.1021/es703102y, 2008.
- Alföldy, B., Loeoev, J. B., Lagler, F., Mellqvist, J., Berg, N., Beecken, J., Weststrate, H., Duyzer, J., Bencs, L., Horemans, B.,
10 Cavalli, F., Putaud, J. P., Janssens-Maenhout, G., Csordas, A. P., Van Grieken, R., Borowiak, A., and Hjorth, J.: Measurements of air pollution emission factors for marine transportation in SECA, *Atmospheric Measurement Techniques*, 6, 1777-1791, 10.5194/amt-6-1777-2013, 2013.
- Almeida, S. M., Silva, A. V., Freitas, M. C., Marques, A. M., Ramos, C. A., Silva, A. I., and Pinheiro, T.: Characterization of dust material emitted during harbour activities by k(0)-INAA and PIXE, *Journal of Radioanalytical and Nuclear Chemistry*,
15 291, 77-82, 10.1007/s10967-011-1279-4, 2012.
- Ault, A. P., Gaston, C. J., Wang, Y., Dominguez, G., Thiemens, M. H., and Prather, K. A.: Characterization of the Single Particle Mixing State of Individual Ship Plume Events Measured at the Port of Los Angeles, *Environmental Science & Technology*, 44, 1954-1961, 10.1021/es902985h, 2010.
- Beirle, S., Platt, U., von Glasow, R., Wenig, M., and Wagner, T.: Estimate of nitrogen oxide emissions from shipping by
20 satellite remote sensing, *Geophysical Research Letters*, 31, 10.1029/2004gl020312, 2004.
- Bengtsson, S., Andersson, K., and Fridell, E.: A comparative life cycle assessment of marine fuels: liquefied natural gas and three other fossil fuels, *Proceedings of the Institution of Mechanical Engineers Part M-Journal of Engineering for the Maritime Environment*, 225, 97-110, 10.1177/1475090211402136, 2011.
- Cabada, J. C., Pandis, S. N., Subramanian, R., Robinson, A. L., Polidori, A., and Turpin, B.: Estimating the secondary organic
25 aerosol contribution to PM_{2.5} using the EC tracer method, *Aerosol Science and Technology*, 38, 140-155, 10.1080/02786820390229084, 2004.
- Campling, P., Janssen, L., Vanherle, K., Cofala, J., Heyes, C., and Sander, R.: Final Report: Specific evaluation of emissions from shipping including assessment for the establishment of possible new emission control areas in European Seas, The Flemish Institute for Technological Research NV, 74, 2013.
- 30 CARB: Final regulation order, fuel sulfur and other operational requirements for ocean-going vessels within California waters and 24 nautical miles of the California baseline, Board, C. A. R., 2009.



- Celo, V., Dabek-Zlotorzynska, E., and McCurdy, M.: Chemical Characterization of Exhaust Emissions from Selected Canadian Marine Vessels: The Case of Trace Metals and Lanthanoids, *Environmental Science & Technology*, 49, 5220-5226, 10.1021/acs.est.5b00127, 2015.
- Contini, D., Gambaro, A., Donato, A., Cescon, P., Cesari, D., Merico, E., Belosi, F., and Citron, M.: Inter-annual trend of the primary contribution of ship emissions to PM_{2.5} concentrations in Venice (Italy): Efficiency of emissions mitigation strategies, *Atmospheric Environment*, 102, 183-190, 10.1016/j.atmosenv.2014.11.065, 2015.
- Cooper, D., and Gustafsson, T.: Methodology for calculating emissions from ships: 1. Update of emission factors, Swedish Environment Research Institute, 2004.
- Cooper, D. A.: Exhaust emissions from ships at berth, *Atmospheric Environment*, 37, 3817-3830, 10.1016/s1352-2310(03)00446-1, 2003.
- Corbett, J. J., Winebrake, J. J., Green, E. H., Kasibhatla, P., Eyring, V., and Lauer, A.: Mortality from ship emissions: A global assessment, *Environmental Science & Technology*, 41, 8512-8518, 10.1021/es071686z, 2007.
- Endresen, O., Sorgard, E., Sundet, J. K., Dalsoren, S. B., Isaksen, I. S. A., Berglen, T. F., and Gravir, G.: Emission from international sea transportation and environmental impact, *Journal of Geophysical Research-Atmospheres*, 108, 10.1029/2002jd002898, 2003.
- Eyring, V., Kohler, H. W., van Aardenne, J., and Lauer, A.: Emissions from international shipping: 1. The last 50 years, *Journal of Geophysical Research-Atmospheres*, 110, 10.1029/2004jd005619, 2005.
- Eyring, V., Isaksen, I. S. A., Berntsen, T., Collins, W. J., Corbett, J. J., Endresen, O., Grainger, R. G., Moldanova, J., Schlager, H., and Stevenson, D. S.: Transport impacts on atmosphere and climate: Shipping, *Atmospheric Environment*, 44, 4735-4771, 10.1016/j.atmosenv.2009.04.059, 2010.
- Finlayson-Pitts, B. J., and Pitts, J. N.: Chemistry of the upper and lower atmosphere: theory, experiments and applications, Academic Press, 2000.
- Fridell, E., Steen, E., and Peterson, K.: Primary particles in ship emissions, *Atmospheric Environment*, 42, 1160-1168, 10.1016/j.atmosenv.2007.10.042, 2008.
- Gao, X. M., Yang, L. X., Cheng, S. H., Gao, R., Zhou, Y., Xue, L. K., Shou, Y. P., Wang, J., Wang, X. F., Nie, W., Xu, P. J., and Wang, W. X.: Semi-continuous measurement of water-soluble ions in PM_{2.5} in Jinan, China: Temporal variations and source apportionments, *Atmospheric Environment*, 45, 6048-6056, 10.1016/j.atmosenv.2011.07.041, 2011.
- Gao, Y., Lee, S. C., Huang, Y., Chow, J. C., and Watson, J. G.: Chemical characterization and source apportionment of size-resolved particles in Hong Kong sub-urban area, *Atmospheric Research*, 170, 112-122, 10.1016/j.atmosres.2015.11.015, 2016.
- Gariazzo, C., Papaleo, V., Pelliccioni, A., Calori, G., Radice, P., and Tinarelli, G.: Application of a Lagrangian particle model to assess the impact of harbour, industrial and urban activities on air quality in the Taranto area, Italy, *Atmospheric Environment*, 41, 6432-6444, 10.1016/j.atmosenv.2007.06.005, 2007.
- Healy, R. M., O'Connor, I. P., Hellebust, S., Allanic, A., Sodeau, J. R., and Wenger, J. C.: Characterisation of single particles from in-port ship emissions, *Atmospheric Environment*, 43, 6408-6414, 10.1016/j.atmosenv.2009.07.039, 2009.



- HKEPD: 2012 Hong Kong Emission Inventory Report, Hong Kong Environmental Protection Department EPD/TR X/14, 26, 2014.
- IMO: Revised MARPOL Annex VI, Organization, I. M., 2008.
- Jalkanen, J. P., Brink, A., Kalli, J., Pettersson, H., Kukkonen, J., and Stipa, T.: A modelling system for the exhaust emissions of marine traffic and its application in the Baltic Sea area, *Atmospheric Chemistry and Physics*, 9, 9209-9223, 10.5194/acp-9-9209-2009, 2009.
- Kattner, L., Mathieu-Ueffing, B., Burrows, J. P., Richter, A., Schmolke, S., Seyler, A., and Wittrock, F.: Monitoring compliance with sulfur content regulations of shipping fuel by in situ measurements of ship emissions, *Atmospheric Chemistry and Physics*, 15, 10087-10092, 10.5194/acp-15-10087-2015, 2015.
- 10 Khoder, M. I.: Atmospheric conversion of sulfur dioxide to particulate sulfate and nitrogen dioxide to particulate nitrate and gaseous nitric acid in an urban area, *Chemosphere*, 49, 675-684, 10.1016/s0045-6535(02)00391-0, 2002.
- Kweon, C. B., Okada, S., Stetter, J. C., Christenson, C. G., Shafer, M. M., Schauer, J. J., and Foster, D. E.: Effect of Fuel Composition on Combustion and Detailed Chemical/Physical Characteristics of Diesel Exhaust, *Jsaes/sae International Spring Fuels and Lubricants Meeting*, 2003,
- 15 Lack, D. A., Cappa, C. D., Langridge, J., Bahreini, R., Buffaloe, G., Brock, C., Cerully, K., Coffman, D., Hayden, K., Holloway, J., Lerner, B., Massoli, P., Li, S.-M., McLaren, R., Middlebrook, A. M., Moore, R., Nenes, A., Nuaaman, I., Onasch, T. B., Peischl, J., Perring, A., Quinn, P. K., Ryerson, T., Schwartz, J. P., Spackman, R., Wofsy, S. C., Worsnop, D., Xiang, B., and Williams, E.: Impact of Fuel Quality Regulation and Speed Reductions on Shipping Emissions: Implications for Climate and Air Quality, *Environmental Science & Technology*, 45, 9052-9060, 10.1021/es2013424, 2011.
- 20 Lai, H. K., Tsang, H., Chau, J., Lee, C. H., McGhee, S. M., Hedley, A. J., and Wong, C. M.: Health impact assessment of marine emissions in Pearl River Delta region, *Marine Pollution Bulletin*, 66, 158-163, 10.1016/j.marpolbul.2012.09.029, 2013.
- Lake, D. A., Tolocka, M. P., Johnston, M. V., and Wexler, A. S.: The character of single particle sulfate in Baltimore, *Atmospheric Environment*, 38, 5311-5320, 10.1016/j.atmosenv.2004.02.067, 2004.
- Lauer, A., Eyring, V., Hendricks, J., Joeckel, P., and Lohmann, U.: Global model simulations of the impact of ocean-going ships on aerosols, clouds, and the radiation budget, *Atmospheric Chemistry and Physics*, 7, 5061-5079, 10.5194/acp-7-5061-2007, 2007.
- 25 Lawrence, S., Sokhi, R., Ravindra, K., Mao, H., Prain, H. D., and Bull, I. D.: Source apportionment of traffic emissions of particulate matter using tunnel measurements, *Atmospheric Environment*, 77, 548-557, 10.1016/j.atmosenv.2013.03.040, 2013.
- Lee, R., Pedley, J., and Hobbs, C.: Fuel Quality Impact on Heavy Duty Diesel Emissions: A Literature Review, *SAE Transactions*, 107, 1952-1970, 10.4271/982649, 1998.
- 30 Li, F. H., Zhang, Y. J., Zhang, J., Yuan, Y., Wu, L., and Mao, H. J.: Characteristics of Particulate and Inorganic Elements of Motor Vehicles Based on a Tunnel Environment, *Huanjing Kexue*, 39, 1014-1022, 10.13227/j.hj.kx.201706226, 2018a.



- Li, X., Li, S., Xiong, Q., Yang, X., Qi, M., Zhao, W., and Wang, X.: Characteristics of PM_{2.5} Chemical Compositions and Their Effect on Atmospheric Visibility in Urban Beijing, China during the Heating Season, *International Journal of Environmental Research and Public Health*, 15, 1924, 2018b.
- Li, X. H., Wang, S. X., Duan, L., Hao, J. M., Li, C., Chen, Y. S., and Yang, L.: Particulate and trace gas emissions from open burning of wheat straw and corn stover in China, *Environmental Science & Technology*, 41, 6052-6058, 10.1021/es0705137, 2007.
- Li, X. H., Wang, S. X., Duan, L., Hao, J. M., and Nie, Y. F.: Carbonaceous Aerosol Emissions from Household Biofuel Combustion in China, *Environmental Science & Technology*, 43, 6076-6081, 10.1021/es803330j, 2009.
- Liu, H., Fu, M. L., Jin, X. X., Shang, Y., Shindell, D., Faluvegi, G., Shindell, C., and He, K. B.: Health and climate impacts of ocean-going vessels in East Asia, *Nature Climate Change*, 6, 1037-+, 10.1038/nclimate3083, 2016.
- Lu, G., Brook, J. R., Alfarra, M. R., Anlauf, K., Leitch, W. R., Sharma, S., Wang, D., Worsnop, D. R., and Phinney, L.: Identification and characterization of inland ship plumes over Vancouver, BC, *Atmospheric Environment*, 40, 2767-2782, 10.1016/j.atmosenv.2005.12.054, 2006.
- Lv, Z., Liu, H., Ying, Q., Fu, M., Meng, Z., Wang, Y., Wei, W., Gong, H., and He, K.: Impacts of shipping emissions on PM_{2.5} air pollution in China, *Atmospheric Chemistry and Physics Discussion*, <https://doi.org/10.5194/acp-2018-540>, 2018.
- Makkonen, U., Virkkula, A., Mantykentta, J., Hakola, H., Keronen, P., Vakkari, V., and Aalto, P. P.: Semi-continuous gas and inorganic aerosol measurements at a Finnish urban site: comparisons with filters, nitrogen in aerosol and gas phases, and aerosol acidity, *Atmospheric Chemistry and Physics*, 12, 5617-5631, 10.5194/acp-12-5617-2012, 2012.
- Matthias, V., Bewersdorff, I., Aulinger, A., and Quante, M.: The contribution of ship emissions to air pollution in the North Sea regions, *Environmental Pollution*, 158, 2241-2250, 10.1016/j.envpol.2010.02.013, 2010.
- McLaren, R., Wojtal, P., Majonis, D., McCourt, J., Halla, J. D., and Brook, J.: NO₃ radical measurements in a polluted marine environment: links to ozone formation, *Atmospheric Chemistry and Physics*, 10, 4187-4206, 10.5194/acp-10-4187-2010, 2010.
- McLaren, R., Wojtal, P., Halla, J. D., Mihele, C., and Brook, J. R.: A survey of NO₂:SO₂ emission ratios measured in marine vessel plumes in the Strait of Georgia, *Atmospheric Environment*, 46, 655-658, 10.1016/j.atmosenv.2011.10.044, 2012.
- Moldanová, J., Fridell, E., Popovicheva, O., Demirdjian, B., Tishkova, V., Faccinnetto, A., and Focsa, C.: Characterisation of particulate matter and gaseous emissions from a large ship diesel engine, *Atmospheric Environment*, 43, 2632-2641, 10.1016/j.atmosenv.2009.02.008, 2009.
- Moreno, N., Alastuey, A., Querol, X., Artinano, B., Guerra, A., Luaces, J. A., Lorente, A., and Basora, J.: Characterisation of dust material emitted during harbour operations (HADA Project), *Atmospheric Environment*, 41, 6331-6343, 10.1016/j.atmosenv.2007.03.028, 2007.
- MOT: Implementation of the Ship Emission Control Area in Pearl River Delta, the Yangtze River Delta and the Bohai Rim (Beijing-Tianjin-Hebei area), Ministry of Transport, C., 8, 2015.
- HYSPLIT (HYbrid Single-Particle Lagrangian Integrated Trajectory): <https://www.arl.noaa.gov/hysplit/hysplit/>, 2013.



- Oanh, N. T. K., Thiansathit, W., Bond, T. C., Subramanian, R., Winijkul, E., and Paw-armart, I.: Compositional characterization of PM_{2.5} emitted from in-use diesel vehicles, *Atmospheric Environment*, 44, 15-22, 10.1016/j.atmosenv.2009.10.005, 2010.
- Ohta, S., and Okita, T.: A CHEMICAL CHARACTERIZATION OF ATMOSPHERIC AEROSOL IN SAPPORO, *Atmospheric Environment Part a-General Topics*, 24, 815-822, 10.1016/0960-1686(90)90282-r, 1990.
- Ostro, B.: Fine particulate air pollution and mortality in two southern California counties, *Environmental Research*, 70, 98-104, 10.1006/enrs.1995.1053, 1995.
- Petzold, A., Weingartner, E., Hasselbach, I., Lauer, P., Kurok, C., and Fleischer, F.: Physical Properties, Chemical Composition, and Cloud Forming Potential of Particulate Emissions from a Marine Diesel Engine at Various Load Conditions, *Environmental Science & Technology*, 44, 3800-3805, 10.1021/es903681z, 2010.
- Press, C. P.: *China Port Yearbook 2017*, 2017.
- Röösli, M., Theis, G., Künzli, N., Staehelin, J., Mathys, P., Oglesby, L., Camenzind, M., and Braun-Fahrländer, C.: Temporal and spatial variation of the chemical composition of PM₁₀ at urban and rural sites in the Basel area, Switzerland, *Atmospheric Environment*, 35, 3701-3713, 10.1016/s1352-2310(00)00511-2, 2001.
- Sinha, P., Hobbs, P. V., Yokelson, R. J., Christian, T. J., Kirchstetter, T. W., and Bruintjes, R.: Emissions of trace gases and particles from two ships in the southern Atlantic Ocean, *Atmospheric Environment*, 37, 2139-2148, 10.1016/s1352-2310(03)00080-3, 2003.
- Sippula, O., Stengel, B., Sklorz, M., Streibel, T., Rabe, R., Orasche, J., Lintelmann, J., Michalke, B., Abbaszade, G., Radischat, C., Groeger, T., Schnelle-Kreis, J., Harndorf, H., and Zimmermann, R.: Particle Emissions from a Marine Engine: Chemical Composition and Aromatic Emission Profiles under Various Operating Conditions, *Environmental Science & Technology*, 48, 11721-11729, 10.1021/es502484z, 2014.
- Song, Y. N.: *Research of emission inventory and emission character of inland and offshore ships*, Beijing Institute of Technology, 2015.
- Tao, L., Fairley, D., Kleeman, M. J., and Harley, R. A.: Effects of Switching to Lower Sulfur Marine Fuel Oil on Air Quality in the San Francisco Bay Area, *Environmental Science & Technology*, 47, 10171-10178, 10.1021/es401049x, 2013.
- Terzi, E., Argyropoulos, G., Bougatioti, A., Mihalopoulos, N., Nikolaou, K., and Samara, C.: Chemical composition and mass closure of ambient PM₁₀ at urban sites, *Atmospheric Environment*, 44, 2231-2239, 10.1016/j.atmosenv.2010.02.019, 2010.
- Thorpe, A., and Harrison, R. M.: Sources and properties of non-exhaust particulate matter from road traffic: A review, *Science of the Total Environment*, 400, 270-282, 10.1016/j.scitotenv.2008.06.007, 2008.
- Tolis, E. I., Saraga, D. E., Filiou, K. F., Tziavos, N. I., Tsiaousis, C. P., Dinas, A., and Bartzis, J. G.: One-year intensive characterization on PM_{2.5} nearby port area of Thessaloniki, Greece, *Environmental Science and Pollution Research*, 22, 6812-6826, 10.1007/s11356-014-3883-7, 2015.



- Tronstad Lund, M., Eyring, V., Fuglestedt, J., Hendricks, J., Lauer, A., Lee, D., and Righi, M.: Global-Mean Temperature Change from Shipping toward 2050: Improved Representation of the Indirect Aerosol Effect in Simple Climate Models, *Environmental Science & Technology*, 46, 8868-8877, 10.1021/es301166e, 2012.
- UNCTAD: World seaborne trade by types of cargo and by group of economies, annual, United Nations Conference on Trade and Development, access: March 2017.
- Viana, M., Hammingh, P., Colette, A., Querol, X., Degraeuwe, B., de Vlieger, I., and van Aardenne, J.: Impact of maritime transport emissions on coastal air quality in Europe, *Atmospheric Environment*, 90, 96-105, 10.1016/j.atmosenv.2014.03.046, 2014.
- Viana, M., Fann, N., Tobias, A., Querol, X., Rojas-Rueda, D., Plaza, A., Aynos, G., Conde, J. A., Fernandez, L., and Fernandez, C.: Environmental and Health Benefits from Designating the Marmara Sea and the Turkish Straits as an Emission Control Area (ECA), *Environmental Science & Technology*, 49, 3304-3313, 10.1021/es5049946, 2015.
- Wang, Y., Zhuang, G. S., Tang, A. H., Yuan, H., Sun, Y. L., Chen, S. A., and Zheng, A. H.: The ion chemistry and the source of PM_{2.5} aerosol in Beijing, *Atmospheric Environment*, 39, 3771-3784, 10.1016/j.atmosenv.2005.03.013, 2005.
- Weckwerth, G.: Verification of traffic emitted aerosol components in the ambient air of Cologne (Germany), *Atmospheric Environment*, 35, 5525-5536, 10.1016/s1352-2310(01)00234-5, 2001.
- Wedepohl, K. H.: THE COMPOSITION OF THE CONTINENTAL-CRUST, *Geochimica Et Cosmochimica Acta*, 59, 1217-1232, 1995.
- Williams, E. J., Lerner, B. M., Murphy, P. C., Herndon, S. C., and Zahniser, M. S.: Emissions of NO_x, SO₂, CO, and HCHO from commercial marine shipping during Texas Air Quality Study (TexAQS) 2006, *Journal of Geophysical Research-Atmospheres*, 114, 10.1029/2009jd012094, 2009.
- Winebrake, J. J., Corbett, J. J., Green, E. H., Lauer, A., and Eyring, V.: Mitigating the Health Impacts of Pollution from Oceangoing Shipping: An Assessment of Low-Sulfur Fuel Mandates, *Environmental Science & Technology*, 43, 4776-4782, 10.1021/es803224q, 2009.
- Winnes, H., and Fridell, E.: Emissions of NO_x and particles from manoeuvring ships, *Transportation Research Part D-Transport and Environment*, 15, 204-211, 10.1016/j.trd.2010.02.003, 2010.
- Winnes, H., Moldanova, J., Anderson, M., and Fridell, E.: On-board measurements of particle emissions from marine engines using fuels with different sulphur content, *Proceedings of the Institution of Mechanical Engineers Part M-Journal of Engineering for the Maritime Environment*, 230, 45-54, 10.1177/1475090214530877, 2016.
- Wojtal, P., Halla, J. D., and McLaren, R.: Pseudo steady states of HONO measured in the nocturnal marine boundary layer: a conceptual model for HONO formation on aqueous surfaces, *Atmospheric Chemistry and Physics*, 11, 3243-3261, 10.5194/acp-11-3243-2011, 2011.
- Xiao, Q., Li, M., Liu, H., Fu, M., Deng, F., Lv, Z., Man, H., Jin, X., Liu, S., and He, K.: Characteristics of marine shipping emissions at berth: profiles for particulate matter and volatile organic compounds, *Atmospheric Chemistry and Physics*, 18, 9527-9545, 10.5194/acp-18-9527-2018, 2018.



- Xing, H., Duan, S. L., Huang, L. Z., and Liu, Q. N.: AIS data-based estimation of emissions from sea-going ships in Bohai Sea areas, *China Environmental Science*, 36, 953-960, 2016.
- Yao, X. H., Chan, C. K., Fang, M., Cadle, S., Chan, T., Mulawa, P., He, K. B., and Ye, B. M.: The water-soluble ionic composition of PM_{2.5} in Shanghai and Beijing, China, *Atmospheric Environment*, 36, 4223-4234, 10.1016/s1352-2310(02)00342-4, 2002.
- 5 Yu, T., Zhao, D., Song, X., and Zhu, T.: NO₂-initiated multiphase oxidation of SO₂ by O₂ on CaCO₃ particles, *Atmospheric Chemistry and Physics*, 18, 6679-6689, 10.5194/acp-18-6679-2018, 2018.
- Zetterdahl, M., Moldanova, J., Pei, X., Pathak, R. K., and Demirdjian, B.: Impact of the 0.1% fuel sulfur content limit in SECA on particle and gaseous emissions from marine vessels, *Atmospheric Environment*, 145, 338-345, 10.1016/j.atmosenv.2016.09.022, 2016.
- 10 Zhang, H., Lang, J., Wen, W., Cheng, S., and Wang, G.: Pollution Characteristics and Regional Transmission of PM_{2.5} in Tangshan, *J. Beijing Univ. Technol. (China)*, 43, 1252-1262, 10.11936/bjutxb2016090045, 2017.
- Zhao, M. J., Zhang, Y., Ma, W. C., Fu, Q. Y., Yang, X., Li, C. L., Zhou, B., Yu, Q., and Chen, L. M.: Characteristics and ship traffic source identification of air pollutants in China's largest port, *Atmospheric Environment*, 64, 277-286, 10.1016/j.atmosenv.2012.10.007, 2013.
- 15

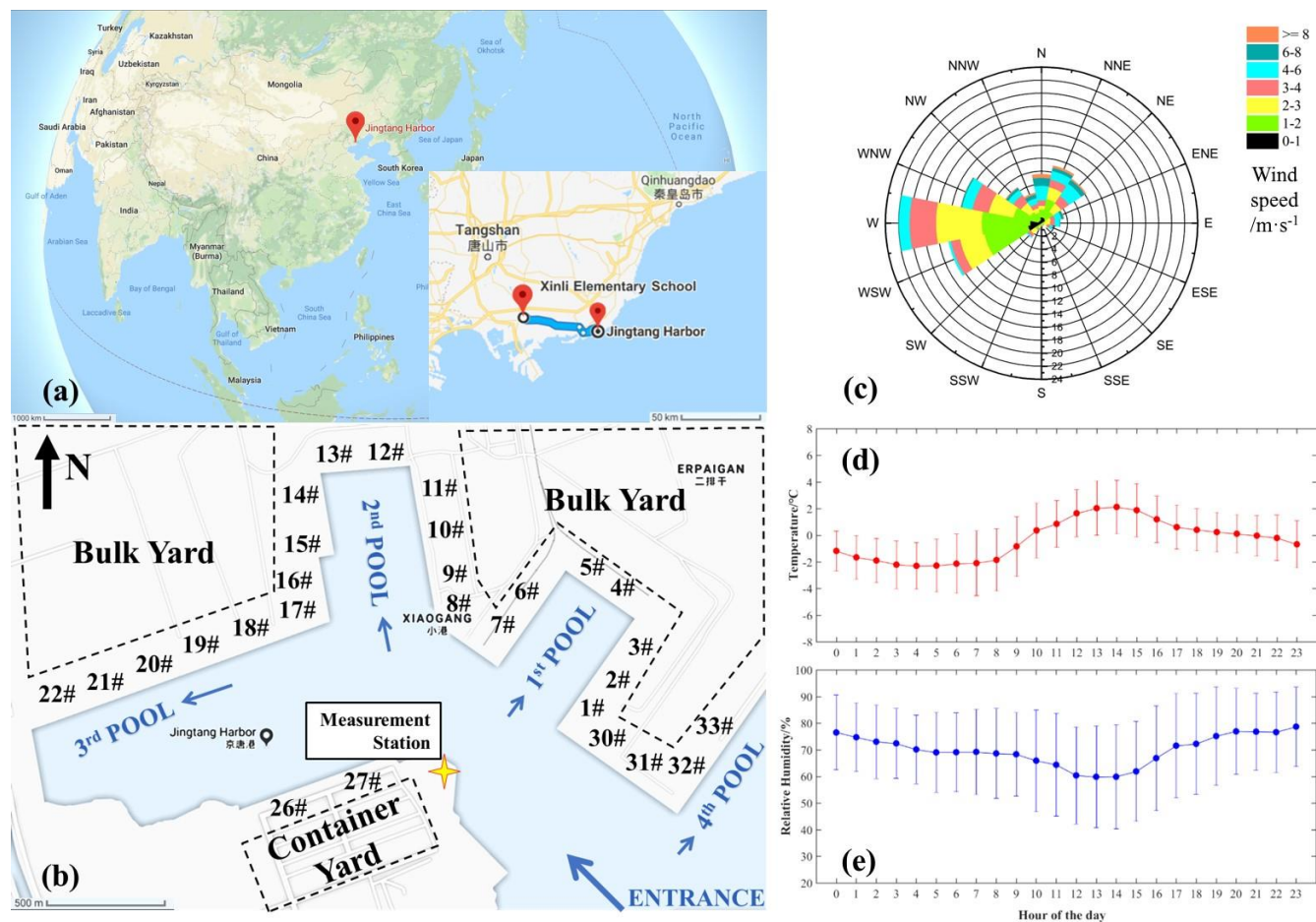


Figure 1: (a) Location of Jingtang Harbor (JT) at a large scale and location of an official air quality monitoring station, Xinli Elementary School (XL) at a smaller scale (map inset). (b) Location of measurement station (yellow marker) and distribution of pools, berths and load areas of the port area. Wind rose (c), daily variation of temperature (d) and relative humidity (e) of measurement station from December 28, 2016 to January 13, 2017.

5

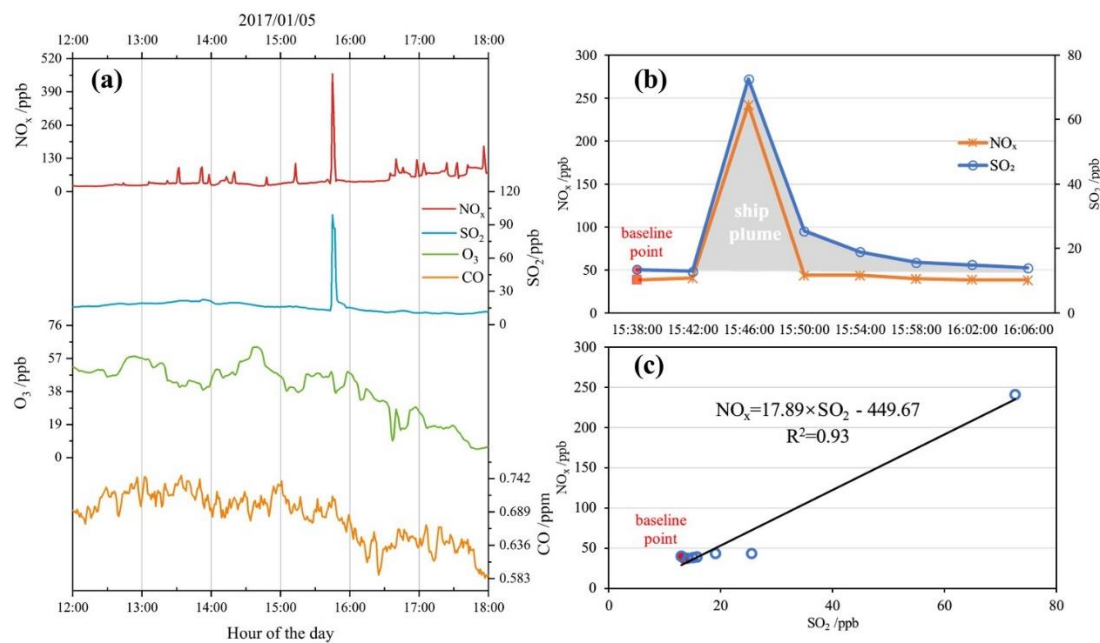


Figure 2: Marine vessel plume #9 showing the (b) ship plume interval identified from (a) NO, SO₂, O₃ and CO concentrations measured in JingTang Harbor (JT) from 12:00 to 18:00, 05 January 2017, and (c) the linear regression method for determination of NO_x/SO₂ ratio.

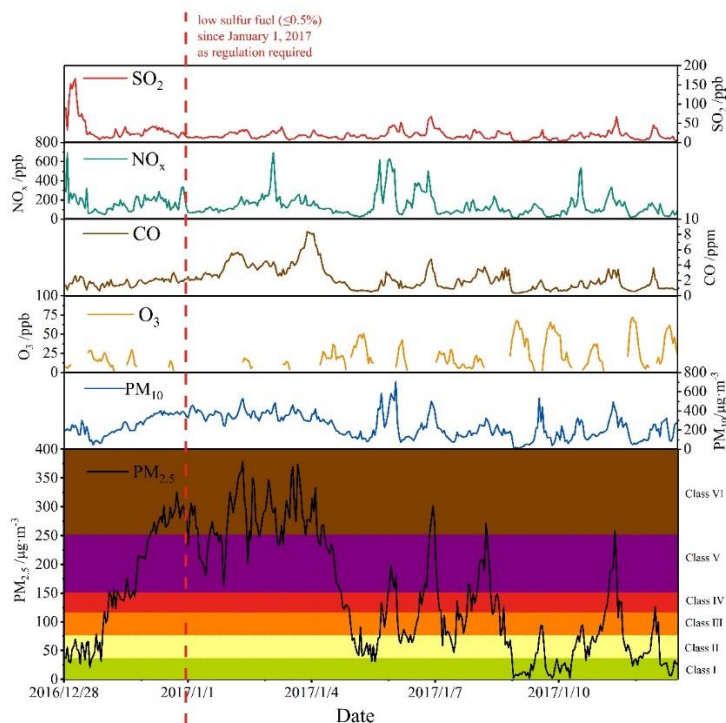




Figure 3: Hourly SO₂, NO_x, CO, O₃, PM₁₀ and PM_{2.5} concentrations measured in JingTang Harbor (JT) from 28 December 2016 to 13 January 2017.

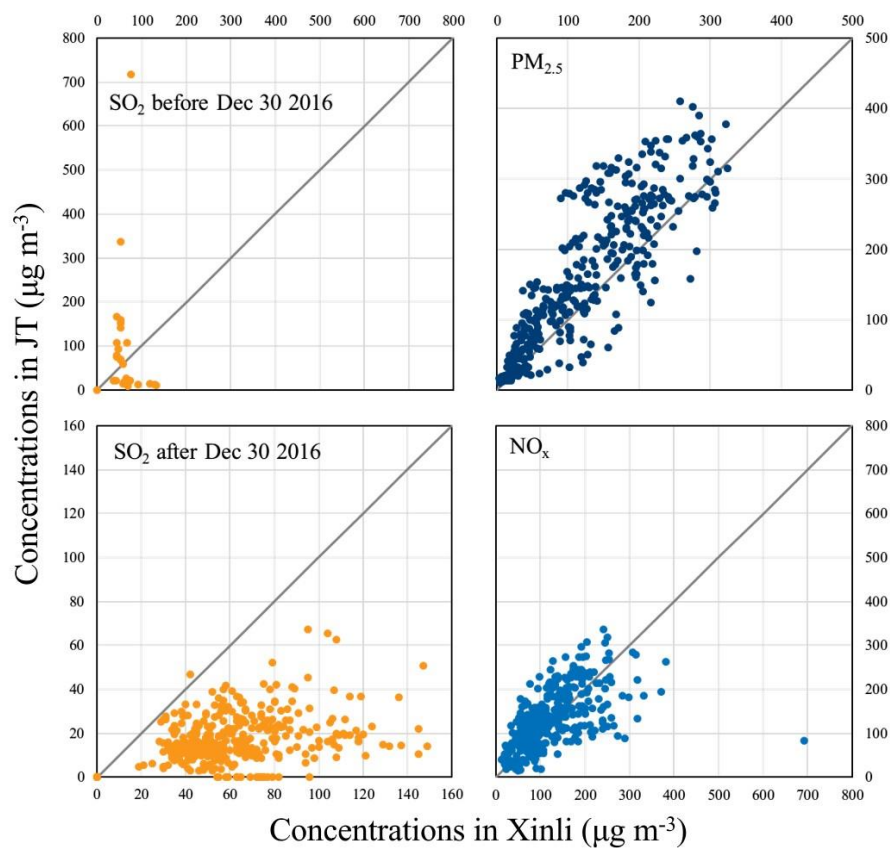


Figure 4: NO_x, SO₂ and PM_{2.5} concentrations in JingTang Harbor (JT) and Xinli Primary School (XL).

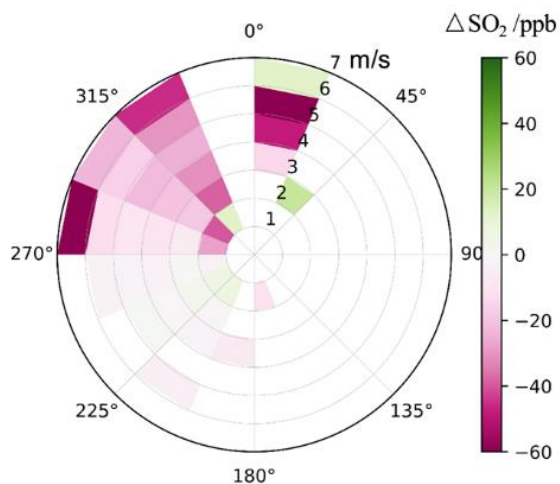




Figure 5: Distribution of differences in SO₂ concentration by wind direction before and after 30 December 2016 in JingTang Harbor. ($\Delta\text{SO}_2 = \text{SO}_2$ after 30 December 2016 - SO_2 before 30 December 2016)

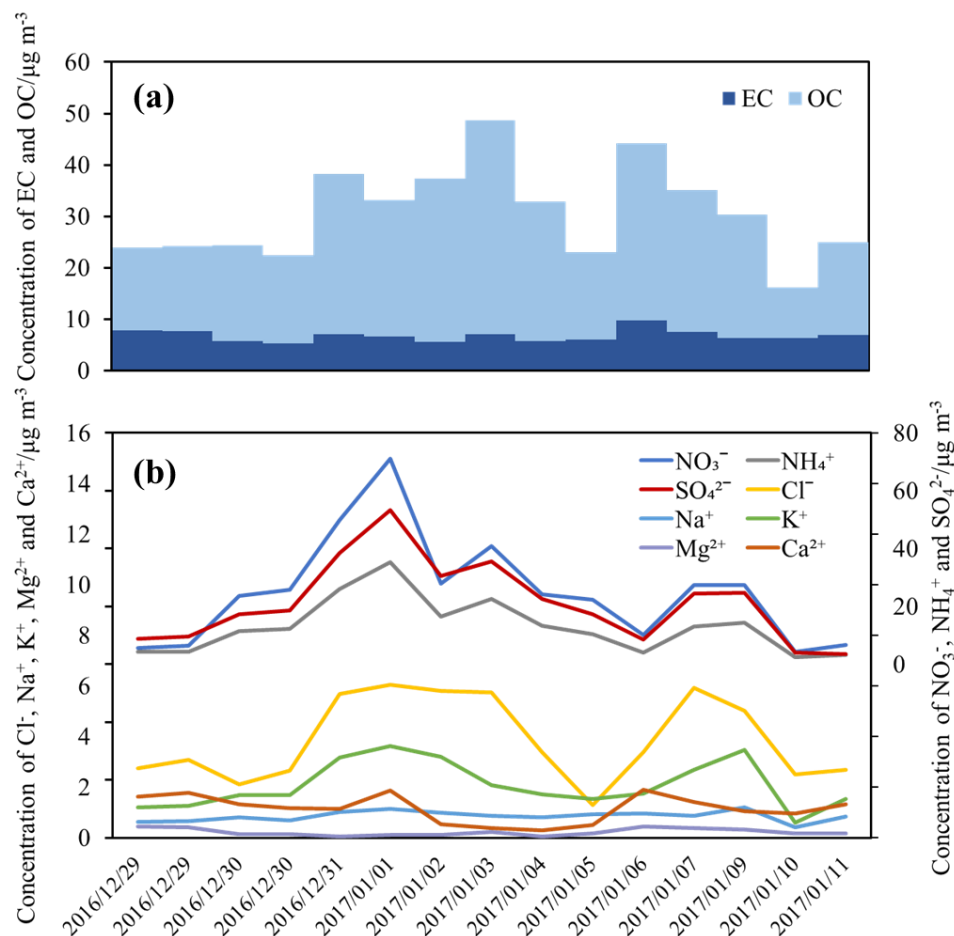


Figure 6: Variation of (a) carbonaceous species and (b) ion species in PM_{2.5}.

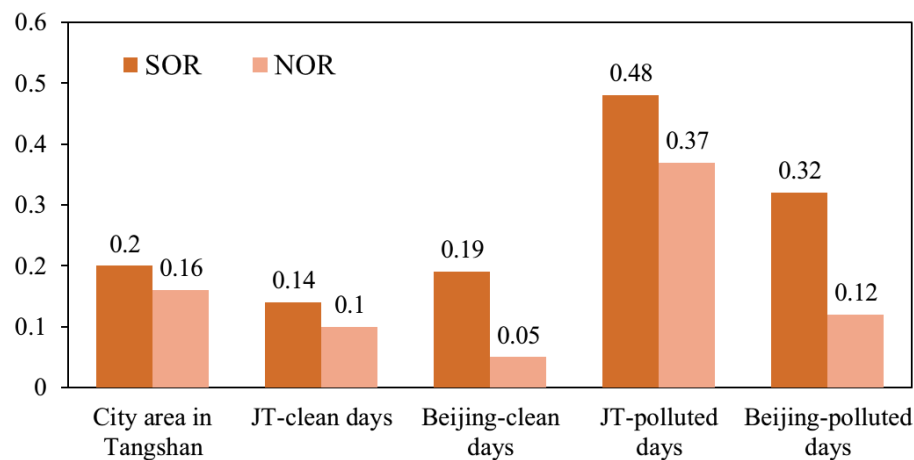




Figure 7: Sulfur Oxidation Rate (SOR) and the Nitrogen Oxidation Rate (NOR) of particles collected in this study, city area of Tangshan (Zhang et al., 2017) and Beijing (Li et al., 2018b).

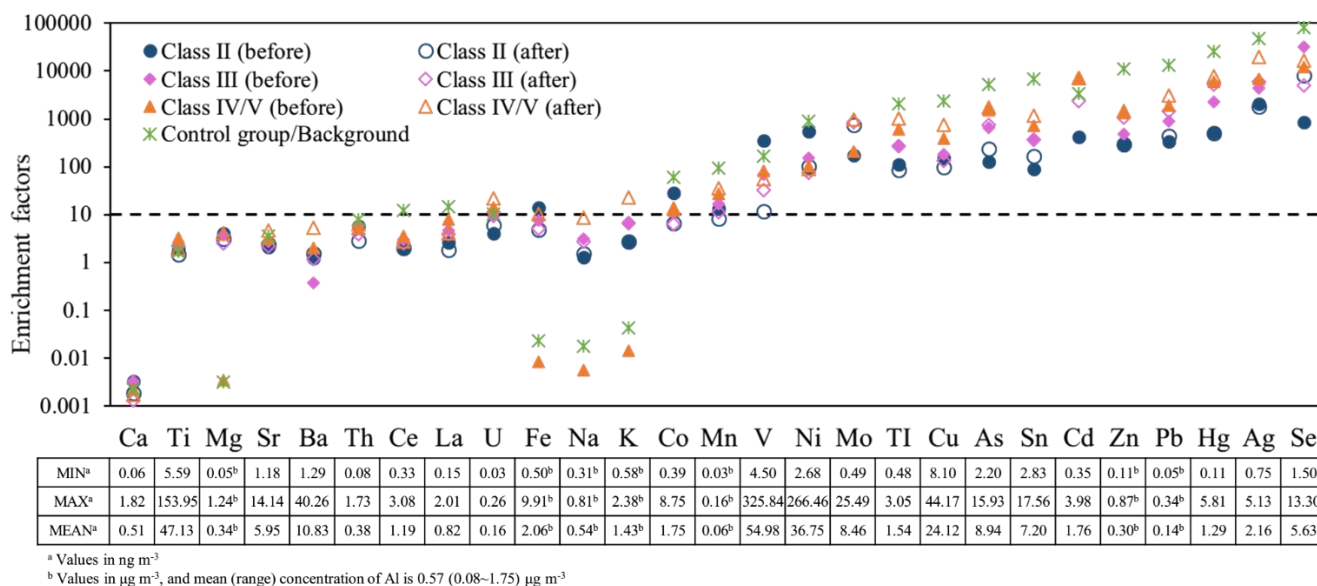


Figure 8: Enrichment factor of elements in PM_{2.5} in JingTang Harbor. The mean, minimum and maximum concentrations of each element are also illustrated.

5

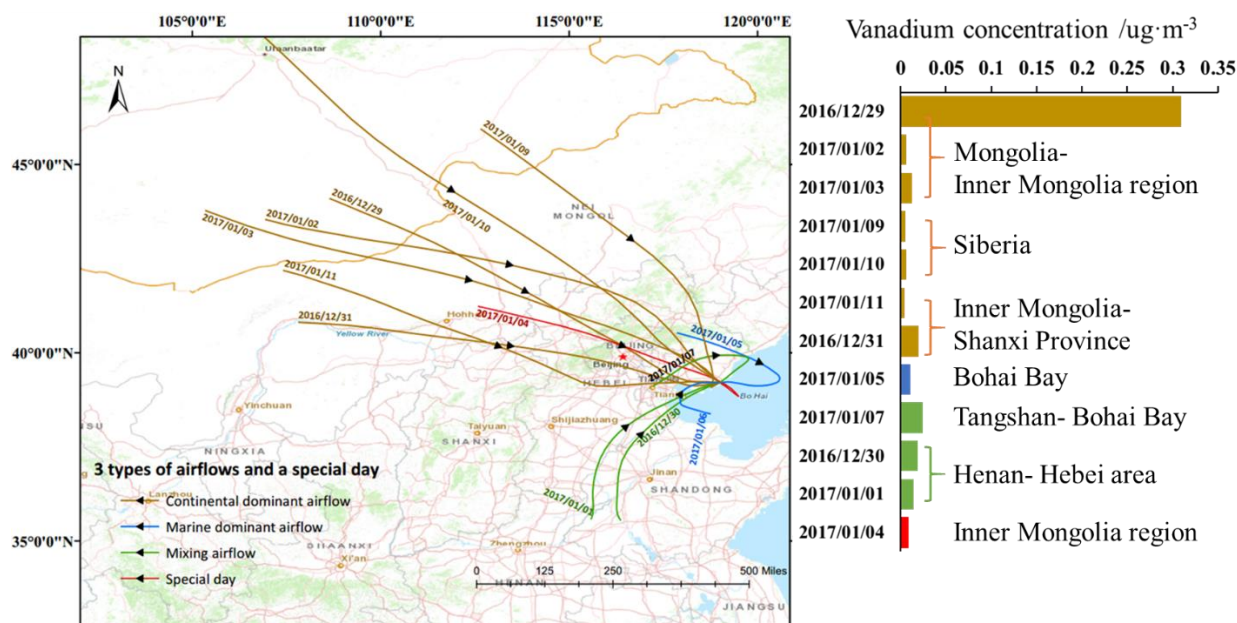


Figure 9: Left: daily trajectories of air masses arriving at JingTang Harbor during the sampling period, with starting dates labelled near the pathways. Right: Concentrations of V in PM_{2.5} of each sample clustered by origin and airflow type.

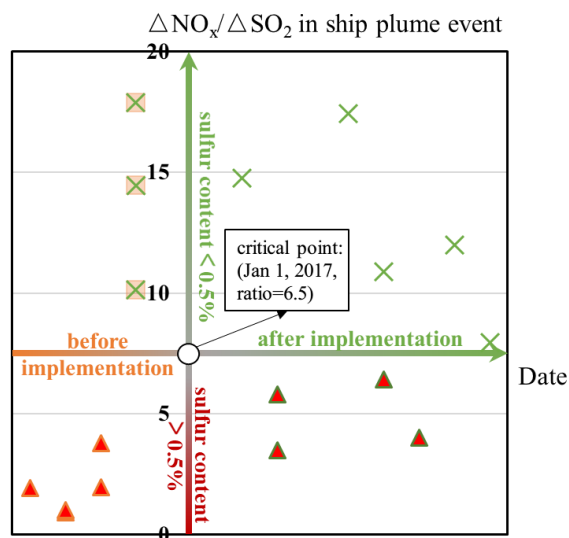


Figure 10: Molar $\Delta\text{NO}_x/\Delta\text{SO}_2$ ratios of all 16 ship plumes. X axis stands for date with positive area meaning time after 1 January 2017. Y axis stands for $\Delta\text{NO}_x/\Delta\text{SO}_2$ ratio with positive area meaning $\text{S}_F < 0.5\%$ in fuel. Plumes within four quadrants are distinguished by different marks.

5

Table 1: Observations of trace gases (ppb) and molar $\Delta\text{NO}_x/\Delta\text{SO}_2$ ratios (ppb ppb^{-1}) in ship plumes

#	Date & Time	Wind Direction	Wind Speed (m s^{-1})	Max NO_x	Max SO_2	Regression $\Delta\text{NO}_x/\Delta\text{SO}_2$	Background ^a NO_x/SO_2	N	R^2
1	Dec 28 23:20~23:44	Northwest	5.26	226	127.6	1.92 ± 0.38	3.16	6	0.83
2	Dec 29 04:08~04:32	West	2.1	239.7	134.7	0.92 ± 0.27	2.06	6	0.68
3	Dec 29 06:52~07:40	West	2.3	277.1	106.5	1.02 ± 0.29	2.06	12	0.51
4	Dec 30 08:36~09:12	West-northwest	1.5	161.5	35.4	1.95 ± 0.4	3.03	9	0.74
5	Dec 30 09:16~09:52	West-northwest	1.8	306.6	60.3	3.79 ± 1.21	3.03	9	0.52
6	Dec 31 07:48~08:12	West	1.2	331.1	42	17.89 ± 2.25	4.99	6	0.93
7	Dec 31 21:40~22:20	West	1.3	551.8	50	10.14 ± 1.55	4.99	10	0.82
8	Dec 31 22:28~23:32	West	1	438.3	29.1	14.48 ± 2.43	4.99	16	0.7
9	Jan 05 15:36~16:08	East-northeast	4.1	242.1	72.6	3.47 ± 0.26	1.29	8	0.96



10	Jan 05 18:24~18:56	East-northeast	2.2	122.9	72.6	5.81 ± 1.25	1.29	8	0.75
11	Jan 08 00:00~00:28	North-northeast	2.5	176.8	17.6	17.45 ± 4.56	3.25	8	0.66
12	Jan 09 04:16~04:48	North	3.7	183.7	28.3	6.43 ± 1.32	1.67	8	0.76
13	Jan 09 23:12~23:56	West	2.8	226	18.9	10.88 ± 1.43	1.67	11	0.85
14	Jan 10 05:08~05:32	North	6.1	158.4	47.9	4.01 ± 1.08	2.13	6	0.72
15	Jan 11 18:16~18:48	West-southwest	1.6	115.3	18	12.00 ± 1.31	2.11	8	0.92
16	Jan 13 14:20~14:42	Northwest	6.4	204.9	32.8	7.95 ± 2.13	2.83	6	0.72

^a concentrations provided by air monitor station in Xinli Primary School (XL).

Table 2: Component of intermediate fuel oil (IFO), marine diesel oil (MDO) and hybrid fuels.

Fuel for main engine	IFOs			Hybrid Fuels				MGOs & MDOs				
	Celo et al. (2015)			Winnes et al. (2016)	Zetterdahl et al. (2016)	Celo et al. (2015)	Winnes et al. (2016)	This study				
	IFO380	IFO180	IFO60					ship A	ship B	ship C		
Density in 15 °C (kg m ⁻³)	988	970.7	957.6	988.7	943.3	982.5	892.8	854.3	846.4	848.2	853.1	846.3
S	2.7	2.23	1.22	0.96	0.58	0.48	0.092	0.119	0.1	0.38	0.08	0.065
C	86.26	85.71	87.22	87.93	87.13	88.4	87.4	86.85	86.29	85.16	84.78	86.83
H	11.26	10.51	11.05	10.68	12.11	10.9	12.8	12.97	13.54	13.07	13.21	13.15
N	0.39	0.41	0.38	0.42	0.3	0.52	0.044	0.026	<0.1	0.027	0.026	0.01
Na	22.66	15.74	--	11	7	--	--	--	<1	1.3	<1	<1
Al	7.06	BD	--	20	16	--	--	--	<1	BD	BD	BD
Ti	2.36	3.12	--	--	--	--	--	--	<1	BD	BD	BD
V	133.8	109.4	38	20	6	5	1	BD	<1	BD	BD	BD
Fe	31.44	20.35	--	9	7	1	2	--	<1	2.7	<1	<1
Ni	63.2	50.3	21	15	9	33	2	BD	<1	BD	BD	BD
Cu	29.51	BD	--	--	--	--	--	--	<1	BD	BD	BD
Zn	2.1	BD	2.2	1	2	--	<1	2.7	<1	BD	BD	BD

BD: below detection limit; --: not reported